

Figure 1. Location of  $z_{EFG}$  axes at N-1 in tautomers (1a) and (1b). The molecule fixed  $F$  system is also shown.

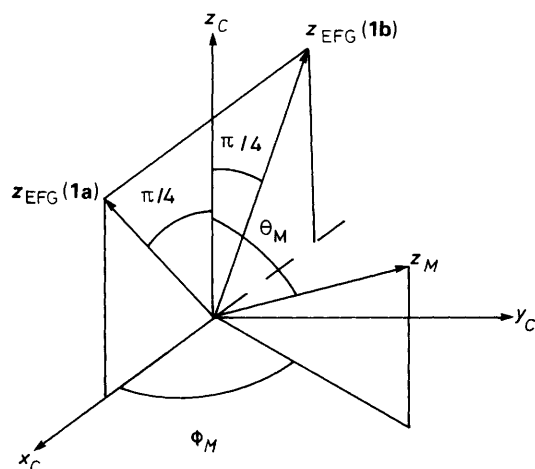


Figure 2. Orientation of the  $z_{EFG}$  axes at N-1 in (1a) and (1b) and of the spinning axis  $z_M$  in the crystal fixed  $C$  system.

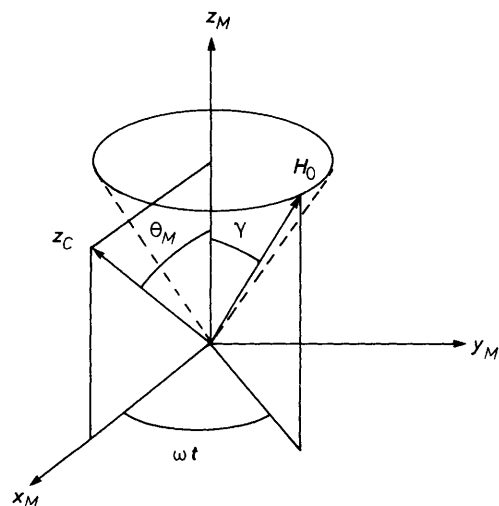


Figure 3. Orientation of the external field and the  $z$  axis of the  $C$  system in the MAS frame used to derive equations (4) and (5). The  $z_C$  axis has been arbitrarily placed in the  $x_M z_M$  plane.

$$S = (9D\chi/20Z)(3\cos^2\beta^D - 1 + \eta\sin^2\beta^D\cos 2\alpha^D) \quad (1)$$

where  $D$  is the dipolar  $^{13}\text{C}$ ,  $^{14}\text{N}$  coupling constant,  $\chi$  is the  $^{14}\text{N}$  quadrupole coupling constant,  $Z$  is the nitrogen Zeeman frequency,  $\eta$  is the asymmetry parameter of the EFG, and  $\beta^D$  and  $\alpha^D$  define the orientation of the internuclear vector  $r_{\text{CN}}$  in the principal axis system (PAS) of the quadrupole tensor.<sup>16</sup> This

approach gives satisfactory results provided that information is known concerning bond distances and angles for the molecule under study, as well as quadrupole parameters for the  $^{14}\text{N}$  nuclei. The angles  $\beta^D$  and  $\alpha^D$  can be estimated if reasonable assumptions are made regarding the arrangement of p orbitals at the nitrogen atoms.<sup>17</sup> Since the  $z_{EFG}$  axis is normally deemed to be coincident with the direction of the lone pair,<sup>21</sup> for the coupling C-1,N-1 in structure (1a) the angle  $\beta^D$  can be set at  $90^\circ$ . On the other hand, the lone pair in (1b) can be assumed to lie in the molecular plane, bisecting the  $\text{R}^1, \text{N}-1, \text{C}-1$  angle. This implies  $\beta^D = 60^\circ$  (Figure 1). Although the exact location of the  $x_{EFG}$  and  $y_{EFG}$  axes is required to define completely the splitting  $S$ , this is not necessary when the EFG has axial symmetry. In what follows, quadrupole tensors will be considered axially symmetric at both chemical sites.

From the analysis of Figure 1 it can be inferred that the proton-transfer reaction induces a corresponding jump of the N-1  $z_{EFG}$  axis between two different sites. This effect, in turn, is likely to contribute to the spin-lattice relaxation of this nitrogen. If  $\chi$  is assumed to adopt the same value both at (1a) and (1b), then the phenomenon is formally equivalent to the well known two-site jumps of deuterons (e.g., as in  $180^\circ$ -flipping phenyl rings). In the present case, however, the change in direction of the  $z_{EFG}$  axis is provided by a rearrangement of bonds instead of by a physical rotation of the C-H bond in space. It has been previously shown that the spin-lattice relaxation time of a  $^2\text{H}$  nucleus jumping between two non-equivalent sites can be given by equation (2)<sup>22</sup> where  $g(\tau, \omega) = \tau/(1 + \omega^2\tau^2)$ ;  $\omega_S = \gamma_S B_0$

$$1/T_1 = \omega_Q^2 p_1 p_2 \sin^2 2\Theta \{ g(\tau, \omega_S) [\cos^2 \theta + \sin^2 \theta \cos^2 \varphi (1 - 4 \cos^2 \theta)] + g(\tau, 2\omega_S) 4 \sin^2 \theta (1 - \sin^2 \theta \cos^2 \varphi) \} \quad (2)$$

( $S = ^2\text{H}$ );  $\omega_Q = 3e^2qQ/4\hbar = 3\chi\pi/$ ;  $p_1$  and  $p_2$  are the populations of sites 1 and 2;  $\tau = (k_{12} + k_{21})^{-1}$ ;  $\Theta$  is the angle made by both orientations of the  $z_{EFG}$  axis with a crystal-fixed axis  $z_C$  and  $\theta$  and  $\varphi$  are the polar and azimuthal angles defining the orientation of the external field in the  $C$  system. In the case under study, where the  $^{14}\text{N}$   $z_{EFG}$  axis undergoes  $90^\circ$  jumps with any chemical exchange act, we can place the  $z_C$  axis as shown in Figure 2, corresponding to  $\Theta = 45^\circ$ .

Increasing  $^{14}\text{N}$  relaxation has been suggested to affect the lines of carbons bonded to nitrogen through the transition rate  $p_{0, \pm 1}$  between the  $|0\rangle$  and  $|\pm 1\rangle$  states.<sup>20</sup> We can identify this rate with the terms in equation (2) containing the spectral density  $g(\tau, \omega_S)$  ( $S = ^{14}\text{N}$ ). Furthermore, a proper expression for the MAS experiment should take into account the time dependence of the angles  $\theta$  and  $\varphi$  due to the sample spinning. In this case,  $p_{0, \pm 1}$  would be as shown in equation (3) where  $p_a$  and  $p_b$  are the populations of tautomers (1a) and (1b) respectively.

$$p_{0, \pm 1} = (9\pi^2 \chi^2 / 4) p_a p_b g(\tau, \omega_S) \{ \cos^2 \theta(t) + \sin^2 \theta(t) \cos^2 \varphi(t) [1 - \cos^2 \theta(t)] \}, \quad (3)$$

If the further assumption is made that the spinning frequency ( $\omega_r/2\pi$ ) is higher than all values of  $p_{0, \pm 1}$  it is possible to average equation (3) in time to obtain the appropriate orientationally dependent equation under MAS conditions.<sup>22</sup> With the direction of the spinning axis defined by  $\theta_M$  and  $\varphi_M$  (Figures 2 and 3), the relations (4) and (5) can be set where  $\gamma$  is the magic angle. Substituting equations (4) and (5) in equation (3) and

$$\cos \theta(t) = \sin \gamma \cos \omega_r t \sin \theta_M + \cos \gamma \cos \theta_M \quad (4)$$

$$\sin \theta(t) \cos \varphi(t) = \cos \gamma \sin \theta_M \cos \varphi_M + \sin \gamma (\sin \omega_r t \cdot \sin \varphi_M - \cos \omega_r t \cos \theta_M \cos \varphi_M), \quad (5)$$

**Table 1.** Values of  $p'_{0,\pm 1}/k$  and  $S'_{av}$  as a function of the angles  $\theta_M$  and  $\varphi_M$ <sup>a</sup>

$\theta_M$	$\varphi_M$	$p'_{0,\pm 1}/10^{-3}k^b$	$S'_{av}/\text{Hz}^c$
0	0	4.8	77
30	0, 180	11.1	81, 90
30	30, 150, 210, 330	9.8	78, 78, 74, 64
30	60, 120, 240, 300	7.2	59, 53, 67, 51
30	90, 270	6.0	48, 56
60	0, 180	11.1	82, 84
60	30, 150, 210, 330	10.4	61, 30, 80, 45
60	60, 120, 240, 300	9.0	40, 8, 76, 42
60	90, 270	8.4	36, 80
90	0	4.8	82 <sup>d</sup>
90	30, 150	6.0	69, 25 <sup>d</sup>
90	60, 120	8.4	79, 35 <sup>d</sup>
90	90	9.6	103 <sup>d</sup>

<sup>a</sup> The following values were used in the calculations:  $\chi = -2$  MHz;  $Z = 7.23$  MHz;  $p_a = p_b = 1/2$  in equation (6);  $r_{CN} = 1.4$  Å;  $\beta^D = 90^\circ$  for site (1a);  $\beta^D = 60^\circ$  for site (1b). <sup>b</sup> Here  $k = \tau^{-1}/2$ . <sup>c</sup> Splittings are given in the order corresponding to  $\varphi_M$ . <sup>d</sup> Due to symmetry considerations, only half of the values are listed for  $\theta_M = 90^\circ$ .

averaging in time leads to equation (6) where ' denotes an orientationally dependent magnitude.

$$p'_{0,\pm 1} = (\pi^2\chi^2/2)p_a p_b g(\tau, \omega_s) [2 - \cos^2\theta_M - \cos^2\varphi_M(1 - \cos^2\theta_M)(1 - 7\cos^2\theta_M)], \quad (6)$$

To illustrate the effect for carbon C-1 in structure (1), the following values will be assumed: C-1, N-1 distance, 1.4 Å;  $\chi(\text{N-1}) = -2$  MHz;  $p_a = p_b = 1/2$ ; and  $\Delta\nu(\text{C-1}) = \nu_b - \nu_a = 500$  Hz [ $\Delta\delta(\text{C-1})$  ca. 20 ppm at 2.3 T], where  $\nu_a$  and  $\nu_b$  are the frequencies of the signals of C-1 in (1a) and (1b). A coalesced line is expected for this carbon when  $\tau^{-1} \gg \Delta\nu(\text{C-1})$ , whereas the collapse of the  $^{13}\text{C}, ^{14}\text{N}$  dipolar splitting will take place for  $p_{0,\pm} \gg S$ . The analysis of equation (6) shows that  $^{14}\text{N}$  quadrupole relaxation effects are expected to be noticeable when the carbon signals corresponding to sites (1a) and (1b) are already coalesced. Therefore, to get an idea of the ability of the quadrupole relaxation in producing the collapse of the residual dipolar splittings, the values of  $p'_{0,\pm 1}$  should be compared with those of the averaged splittings  $S'_{av} = (1/2)(S'_a + S'_b)$  where  $S'_a$  and  $S'_b$  are the partitions predicted for C-1 in the tautomeric forms (1a) and (1b) respectively. The latter must be evaluated at different orientations  $\theta_M$  and  $\varphi_M$ , and this can be done by using the previously reported expression (7),<sup>18</sup>  $\zeta_{zi}$  and  $\zeta_r$  being the

$$S'_i = (9D\chi/4Z) \{ \cos^2\beta_i^D - (1/6)[1 + \cos^2\zeta_{zi} + \cos^2\zeta_r \cdot (1 - 9\cos^2\zeta_{zi}) + 2(\cos\beta_i^D + \cos\zeta_{zi}\cos\zeta_r)^2] \} \quad (7)$$

angles made by the  $z_{\text{EFG}}$  axis at each site and the  $r_{\text{CN}}$  vector with the spinning axis respectively. From Figures 1 and 2, the value of  $\cos\zeta_{za}$ ,  $\cos\zeta_{zb}$ , and  $\cos\zeta_r$  can be shown to be:

$$\cos\zeta_{za} = \sqrt{2}(\cos\theta_M + \sin\theta_M\cos\varphi_M)/2 \quad (8)$$

$$\cos\zeta_{zb} = \sqrt{2}(\cos\theta_M - \sin\theta_M\cos\varphi_M)/2 \quad (9)$$

$$\cos\zeta_r = \sqrt{2}\cos\theta_M/4 - \sin\theta_M(\sqrt{2}\cos\varphi_M/4 + \sqrt{3}\sin\varphi_M/2). \quad (10)$$

Table 1 shows values of  $S'_{av}$  and  $p'_{0,\pm 1}$  for a regime in which  $\tau^2\omega_s^2 \gg 1$ , as a function of  $\theta_M$  and  $\varphi_M$ . Most of the splittings are expected to be collapsed when  $k > \text{ca. } 10^4 \text{ s}^{-1}$ . On the other hand, analysis of the region  $\tau^2\omega_s^2 \ll 1$  shows that the  $^{14}\text{N}$

relaxation effect will no longer be effective for residence times smaller than ca.  $10^{-11}$  s. Thus a self-decoupling phenomenon is expected in the range  $10^4 < k < 10^{11} \text{ s}^{-1}$ .

Effects of  $^{14}\text{N}$  relaxation on carbon lines affected by dipolar coupling to nitrogen have been previously analysed using an analogy with chemical exchange.<sup>20</sup> In this simple, stochastic-Liouvillian approach carbons at each chemical site that are associated with different  $^{14}\text{N}$  spin states are assumed to undergo exchange with rates given by the transition probabilities among nitrogen eigenstates.<sup>23</sup> In the present case a four-sites problem may be adequate, with frequencies  $\nu_a + 2S'_a/3$ ,  $\nu_a - S'_a/3$ ,  $\nu_b + 2S'_b/3$ , and  $\nu_b - S'_b/3$ , and populations in the ratio 1:2:1:2. Since the  $S'$  are orientationally dependent, the final line shape should be calculated by adding the individual ones arising from all orientations in space. This can be done by scanning the angles  $\theta_M$  and  $\varphi_M$  as is usual in the computation of NMR powder patterns. The results are presented in Figure 4 in comparison with a similar calculation involving no  $^{14}\text{N}$  quadrupole relaxation. Both columns are comparable in the slow exchange limit, where the residual coupling to  $^{14}\text{N}$  is clearly noticed. When the carbon lines coalesce, however, a self-decoupling induced by the mechanism under study is observed [Figure 4 (a),(b)]. Not shown in this figure are the line shapes for exchange rates higher than ca.  $10^{11} \text{ s}^{-1}$ . Within the present  $^{14}\text{N}$  relaxation model they exhibit  $^{13}\text{C}, ^{14}\text{N}$  residual coupling effects identical with those obtained by considering an infinitely long  $T_{1\text{N}}$ .

The above discussion was explicitly based on the existence of a double-minimum potential for the proton transfer process. However, it is also possible for the N-H proton to be confined to a single-minimum potential structure (1c). In this case, the quadrupole-induced relaxation may not be favourable for the nitrogen nuclei, allowing the  $^{13}\text{C}, ^{14}\text{N}$  splittings to be observed. It is interesting to compare the magnitude of the predicted splitting for the signal of C-1 in structure (1c) with that calculated for a fast equilibrium (1a) = (1b) in the absence of  $^{14}\text{N}$  relaxation effects. Thus attention will be focussed on the dynamically averaged splitting  $S_{av} = p_a S_a + p_b S_b$  where  $S$  now denotes the distance between the centres of mass of the two lines generated by the residual dipolar coupling to N-1, as given by equation (1). If the values of  $\beta^D$  assumed above for each tautomeric structure are introduced in equation (1), one obtains:

$$S_{av} = -(9D\chi/80Z)(1 + 3p_a) \quad (11)$$

This  $S_{av}$  can also be seen as arising from an average quadrupole tensor characterized by  $\chi_{av}$  and, in general, by  $\eta_{av}$ :

$$S_{av} = (9D\chi_{av}/20Z)(3\cos^2\beta_{av}^D - 1 + \eta_{av}\sin^2\beta_{av}^D\cos 2\alpha_{av}^D) \quad (12)$$

Assuming that the  $\text{R}^1\text{N-1,C-1}$  moiety has an approximate plane of symmetry ( $y_F z_F$  in this case; see Figure 1), the average tensor at N-1 will be diagonal in the  $F$ -axis system, with principal values given by  $-(1/2)\chi$  along  $x_F$ ,  $(-p_a/2 + p_b)\chi$  along  $y_F$ , and  $(p_a - p_b/2)\chi$  along  $z_F$ . Plots of these EFG components are shown in Figure 5, which can be divided into four regions according to the labelling of  $x_{\text{EFG}}$ ,  $y_{\text{EFG}}$ , and  $z_{\text{EFG}}$  axes. Table 2 shows those assignments, together with the values of  $\chi_{av}$ ,  $\eta_{av}$ , and the resulting angles  $\beta_{av}^D$  and  $\alpha_{av}^D$ . As expected, splittings calculated by introducing the average values in equation (12) conform to the results given by equation (11).

In a single-minimum potential structure N-1 will exhibit a unique EFG tensor, with properties intermediate between those at sites (1a) and (1b). An elegant method for connecting quadrupole parameters and directions of the principal axes of the quadrupole tensor to the  $^{14}\text{N}$  p-orbital populations has been described by Vega.<sup>24</sup> He related the properties of the EFG tensor to four effective charges  $Q_i$  ( $i = 1, 2, 3, 4$ , where  $\varphi_1$  and  $\varphi_2$

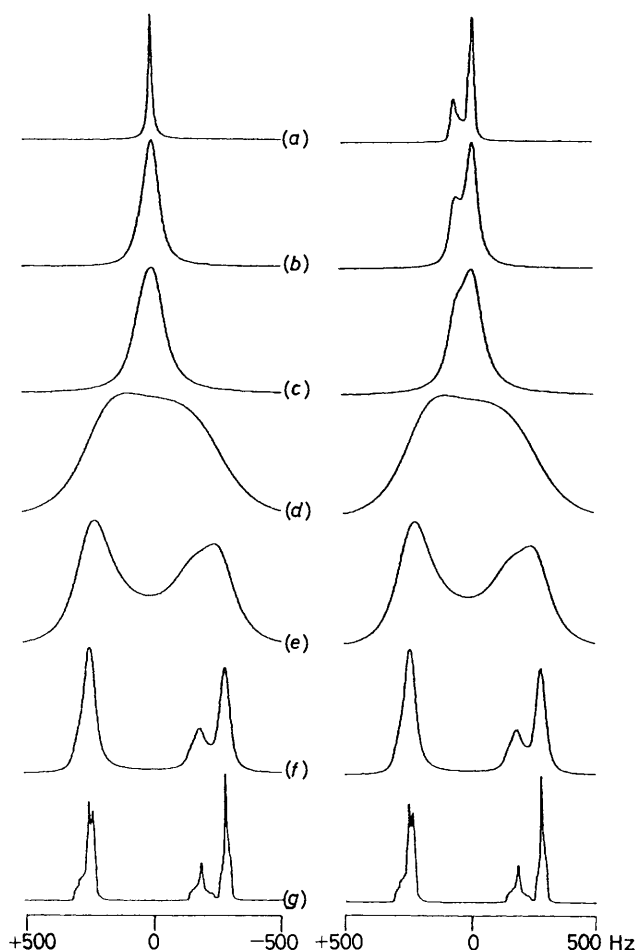


**Figure 4.** Left column: calculated line shapes for carbon C-1 in a structure showing proton migration between (1a) and (1b) when  $^{14}\text{N}$  spin-lattice relaxation is present. A four-sites chemical exchange analogy has been used, with site frequencies given by  $\nu_1 = +250 \text{ Hz} + 2S'_6/3$ ,  $\nu_2 = +250 \text{ MHz} - S'_6/3$ ,  $\nu_3 = -250 \text{ Hz} + 2S'_7/3$ , and  $\nu_4 = -250 \text{ Hz} - S'_7/3$ , and site populations in the ratio 1:2:1:2. Rate constants are  $k_{13} = k_{31} = k_{24} = k_{42} = k$ ,  $k_{14} = k_{41} = k_{23} = k_{32} = 0$ , and  $k_{21} = k_{43} = k_{12}/2 = k_{34}/2 = p'_{0,\pm 1}$ . Values of  $k = \tau^{-1}/2$  used in the simulations are (in  $\text{s}^{-1}$ ): (a)  $5.10^4$ ; (b)  $10^2$ ; (c)  $5.10^3$ ; (d)  $10^3$ ; (e)  $5.10^2$ ; (f)  $10^2$ ; and (g) 10. Splittings  $S'$  were calculated using equations (7)–(10), with  $r(\text{C-1,N-1}) = 1.4 \text{ \AA}$ ,  $\chi(\text{N-1}) = -2 \text{ MHz}$ ,  $Z = 7.23 \text{ MHz}$ ,  $\beta^D = 90^\circ$  at (1a), and  $\beta^D = 60^\circ$  at (1b), whereas the rates  $p'_{0,\pm 1}$  were calculated through equation (6) introducing  $p_a = p_b = 1/2$  and the corresponding value of  $k$ . The signals shown are a superposition of all line shapes arising after scanning the angles  $\theta_M$  and  $\varphi_M$  and giving each signal a weight equal to  $\sin\theta_M$ . Right column: predicted line shapes in the absence of quadrupole relaxation for the nitrogen nuclei. The parameters used are the same as those in the left column, except that in this case  $k_{12} = k_{21} = k_{34} = k_{43} = 0$ . Both columns are similar in the slow exchange range. For  $k > 10^4 \text{ s}^{-1}$  the left column shows a self-decoupling phenomenon. Not shown in this figure are the line shapes for  $k > 10^{11} \text{ s}^{-1}$ , which both in the presence and absence of  $^{14}\text{N}$  relaxation are similar than that presented in (a), right column.

denote  $\text{sp}^2$  hybrids directed towards  $\text{R}^1$  and C-1,  $\varphi_3$  points along  $y_F$  and  $\varphi_4$  along  $z_F$ ). These effective charges are proportional to both the occupation numbers  $a_i$  and the p character of each hybrid. A link between this method and the double-minimum potential model can be set if the properties of the population averaged tensor are ascribed to the quadrupole interaction occurring in (1c). The ratio between the populations  $p_a$  and  $p_b$  can be equated to the corresponding one between the effective charges in hybrids  $\varphi_4$  and  $\varphi_3$ , equation (13) where the

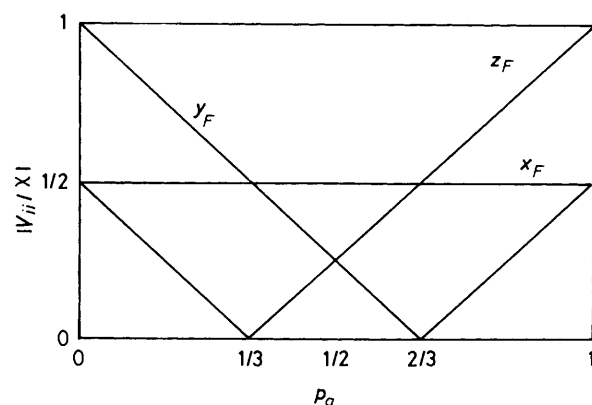


**Figure 5.** Plot of the EFG principal components at N-1 along the  $x_F$ ,  $y_F$ , and  $z_F$  axes as a function of  $p_a$ . The values of  $|V_{ij}/\chi|$  were obtained by averaging the quadrupole tensors at (1a) and (1b) according to the site populations.

$$\frac{p_a}{p_b} = \frac{3(a_4 - a_1)}{2(a_3 - a_1)} \quad (13)$$

factor (3/2) accounts for the different p characters of  $\varphi_4$  and  $\varphi_3$ . With this definition, Vega's reduced charge  $c = (a_1 - a_4)/(a_3 - a_4)$  becomes:

$$c = \frac{2p_a}{5p_a - 3} \quad (14)$$

Values of  $c$  in each of the four regions of Figure 5 are given in Table 2. Not only are they coincident with those derived by Vega,<sup>24</sup> but also the labellings of axes are in agreement. It is interesting to note in this regard the experimental results reported by Garcia *et al.*<sup>25</sup> on substituted imidazoles. For =N– groups, increasing hydrogen bonding causes  $\chi$  to decrease and  $\eta$  to increase, in agreement with predictions based on Figure 5 and Table 2 in the region near  $p_a = 0$ . For N–H groups it was found that  $\chi$  decreases and  $\eta$  increases with stronger hydrogen bonding, up to a point where the introduction of very strong donor species causes  $\chi$  to reverse sign, and the  $y_{\text{EFG}}$  and  $z_{\text{EFG}}$  axes to interchange their directions.<sup>25</sup> This agrees with the analysis of Figure 5 and Table 2 in the region  $1/2 < p_a \leq 1$ . Thus it is reasonable to expect a splitting at C-1 in the static model (1c) as given by equation (11), with  $p_a$  measuring the degree of asymmetry of the single proton potential.

These results may be useful for the distinction of double- and single-minimum energy profiles when average NMR. lines are obtained at all accessible temperatures. In the appropriate range of exchange rates, a tautomeric equilibration may lead to the self-decoupling of the carbons adjacent to the exchanging nitrogens. In a single resonance structure, on the other hand, carbon lines should be split by an amount equivalent to that calculated as the population average of the partitions predicted for the extreme tautomers.

Available experimental data concerning the phenomenon under discussion are scarce. Few  $^{14}\text{N}$ -containing solid samples showing proton exchange reactions have been hitherto studied by  $^{13}\text{C}$  CPMAS spectroscopy. Residual dipolar coupling effects have been invoked to account for the solid state  $^{13}\text{C}$  NMR spectra of certain free-base porphyrins in the slow regime.<sup>4a,b</sup> In the fast exchange limit, however, the large line width of the signals precluded the observation of clear self-decoupling effects. Recent results derived from CPMAS analyses of azo dyes indicated the possibility of collapsed splittings due to a fast  $\text{N} \cdots \text{O}$  proton-transfer reaction.<sup>26</sup> Work is in progress in other nitrogen-containing materials in order to support the conclusions reached in the present paper.

**Table 2.** Values of  $\chi_{av}$ ,  $\eta_{av}$ , reduced charge,  $c$ ,  $\beta_{av}^D$ , and  $\alpha_{av}^D$  and labelling of EFG axes in the four regions of Figure 5.

	Range of $p_a$			
	$0 \leq p_a \leq 1/3$	$1/3 < p_a \leq 1/2$	$1/2 < p_a \leq 2/3$	$2/3 < p_a \leq 1$
$\chi_{av}/\chi$	$(2 - 3p_a)/2$	$-1/2$	$-1/2$	$(3p_a - 1)/2$
$\eta_{av}$	$3p_a/(2 - 3p_a)$	$3(1 - 2p_a)$	$3(2p_a - 1)$	$(3 - 3p_a)/(3p_a - 1)$
Range of $c^a$	$0 \geq c \geq -1/2$	$-1/2 > c \geq -2$	$-2 > c; c \geq 4^b$	$4 > c \geq 1$
$\beta_{av}^D$	$90^\circ$	$30^\circ$	$30^\circ$	$60^\circ$
$\alpha_{av}^D$	$60^\circ$	$0$	$90^\circ$	$90^\circ$
$x_{EFG}$	$z_F$	$z_F$	$y_F$	$y_F$
$y_{EFG}$	$x_F$	$y_F$	$z_F$	$x_F$
$z_{EFG}$	$y_F$	$x_F$	$x_F$	$z_F$

<sup>a</sup> This reduced charge has been previously defined by Vega (ref. 24) as  $c = (a_1 - a_4)/(a_3 - a_4)$ . <sup>b</sup> The value of  $c$  passes through  $\pm \infty$  in this range.

## Conclusions

A model has been discussed which allows the study of the collapse of  $^{13}\text{C}$ ,  $^{14}\text{N}$  residual dipolar splittings in  $^{13}\text{C}$  CPMAS spectroscopy of chemically exchanging  $^{14}\text{N}$ -containing materials. The results show that a proton migration is likely to induce a nitrogen spin-lattice relaxation fast enough to decouple the carbon resonances from the effect of adjacent nitrogen atoms. A simple approach has been used to analyse the dependence of the signal shapes on rate constants, based on an analogy of the self-decoupling phenomenon with chemical exchange. In addition, the consequences of the existence of a single-minimum potential have been discussed. Simple ideas based on Vega's method for relating quadrupole parameters to the occupation numbers of the nitrogen p orbitals have been applied. It has been shown that carbon splittings should be observed in non-exchanging systems with different degrees of asymmetry in the proton potential, with magnitudes given by a population average of the splittings calculated for the extreme tautomeric structures.

## Acknowledgements

Support from Consejo Nacional de Investigaciones Científicas y Técnicas (CONICET) and from the University of Rosario is gratefully acknowledged.

## References

- 1 P. Dauber and A. Hagler, *Acc. Chem. Res.*, 1980, **13**, 105.
- 2 J. A. Sussman, *Mol. Cryst. Liq. Cryst.*, 1972, **18**, 39.
- 3 D. Y. Curtin and I. C. Paul, *Chem. Rev.*, 1981, **81**, 525.
- 4 (a) L. Frydman, A. C. Olivieri, L. E. Diaz, B. Frydman, F. G. Morin, C. L. Mayne, D. M. Grant, and A. D. Adler, *J. Am. Chem. Soc.*, 1988, **110**, 336; (b) L. Frydman, A. C. Olivieri, L. E. Diaz, A. Valasinas, and B. Frydman, *ibid.*, 1988, **110**, 5651; (c) B. Wehrle, H.-H. Limbach, M. Kocher, O. Ermer, and E. Vogel, *Angew. Chem.*, 1987, **26**, 934; (d) B. Wehrle, H. Zimmermann, and H.-H. Limbach, *J. Am. Chem. Soc.*, 1988, **110**, 7014.
- 5 F. H. Herbstein, M. Kapon, G. M. Reisner, M. S. Lehman, R. B. Kress, R. B. Wilson, W.-I. Shiau, E. N. Duesler, I. C. Paul, and D. Y. Curtin, *Proc. R. Soc. London, Ser. A*, 1985, **399**, 295; W.-I. Shiau, E. N. Duesler, I. C. Paul, D. Y. Curtin, W. G. Blann, and C. A. Fyfe, *J. Am. Chem. Soc.*, 1980, **102**, 4546.
- 6 N. M. Szeverenyi, M. J. Sullivan, and G. E. Maciel, *J. Magn. Reson.*, 1982, **47**, 462.
- 7 S. Nagaoka, N. Hirota, T. Matsushita, and K. Nishimoto, *Chem. Phys. Lett.*, 1982, **92**, 498; W. Hayashi, J. Umemura, S. Kato, and K. Morokuma, *J. Chem. Phys.*, 1984, **88**, 1330.
- 8 G. C. Pimentel and A. L. McClellan, 'The Hydrogen Bond,' W. H. Freeman, San Francisco, 1960.
- 9 W. C. Hamilton and J. A. Ibers, 'Hydrogen Bonding in Solids,' W. A. Benjamin, New York, 1968.
- 10 'The Hydrogen Bond. Recent Developments in Theory and Experiments,' eds. P. Schuster, G. Zundel, and C. Sandorfy, North Holland, Amsterdam, 1976, vol. 1-3.
- 11 I. Olovsson and P. Jonsson, in ref. 10, vol. 1, ch. 8.
- 12 J. C. Speakman, 'Acid Salts of Carboxylic Acids, Crystals with some "Very Short Hydrogen Bonds",' in 'Structure and Bonding,' eds. J. D. Dunitz *et al.*, Springer-Verlag, Berlin, 1972, p. 141-199.
- 13 A. Naito, S. Ganapathy, and C. A. McDowell, *J. Chem. Phys.*, 1981, **74**, 5393.
- 14 P. M. Zumbulyadis, P. M. Henrichs, and R. H. Young, *J. Chem. Phys.*, 1981, **75**, 1603.
- 15 J. G. Hexem, M. H. Frey, and S. J. Opella, *J. Chem. Phys.*, 1982, **77**, 3847.
- 16 A. C. Olivieri, L. Frydman, and L. E. Diaz, *J. Magn. Reson.*, 1987, **75**, 50.
- 17 A. C. Olivieri, L. Frydman, M. Grasselli, and L. E. Diaz, *Magn. Reson. Chem.*, 1988, **26**, 281.
- 18 A. C. Olivieri, L. Frydman, M. Grasselli, and L. E. Diaz, *Magn. Reson. Chem.*, 1988, **26**, 615.
- 19 P. Jonsen, *J. Magn. Reson.*, 1988, **77**, 348.
- 20 A. C. Olivieri, *J. Magn. Reson.*, 1989, **82**, 342.
- 21 E. A. C. Lucken, 'Nuclear Quadrupole Coupling Constants,' Academic Press, London, 1969, ch. 9.
- 22 D. A. Torchia and A. Szabo, *J. Magn. Reson.*, 1982, **49**, 107.
- 23 J. A. Pople, *Mol. Phys.*, 1968, **1**, 168.
- 24 S. Vega, *J. Chem. Phys.*, 1974, **60**, 3884.
- 25 M. L. S. Garcia, J. A. S. Smith, P. M. G. Bavin, and C. R. Ganellin, *J. Chem. Soc., Perkin Trans. 2*, 1983, 1391.
- 26 A. C. Olivieri, R. Wilson, I. C. Paul, and D. Y. Curtin, *J. Am. Chem. Soc.*, 1989, **111**, 5525.

Received 19th June 1989; Paper 9/02563D